RESEARCH ARTICLE

In vivo observation of cerebral microcirculation after experimental subarachnoid hemorrhage in mice

Xiao-mei Yang[1], Xu-hao Chen[2], Jian-fei Lu[1], Chang-man Zhou[1], Jing-yan Han[3,*], Chun-hua Chen[1,*]
1 Department of Human Anatomy and Embryology, Peking University Health Science Center, Beijing, China
2 School of Basic Medical Sciences, Peking University Health Science Center, Beijing, China
3 Tasly Microcirculation Research Center, Peking University Health Science Center, Beijing, China

Funding: *This study was supported by the National Natural Science Foundation of China, No. 81100856.*

Graphical Abstract

***In vivo* changes in cerebral microcirculation in the early stage of subarachnoid hemorrhage (SAH) in mice**

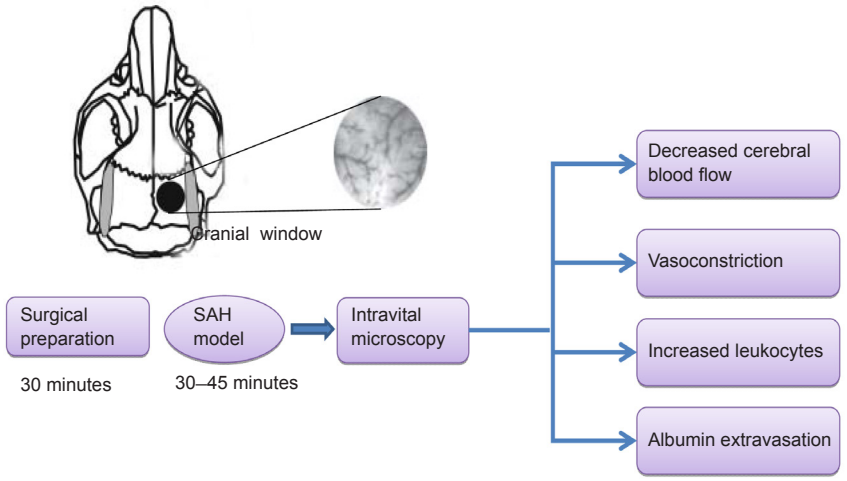

***Correspondence to:**
Chun-hua Chen, M.D., Ph.D. or Jing-yan Han, cch@bjmu.edu.cn.

orcid:
0000-0002-8502-8189 (Chun-hua Chen)

doi: *10.4103/1673-5374.228728*

Accepted: *2017-11-30*

Abstract

Acute brain injury caused by subarachnoid hemorrhage is the major cause of poor prognosis. The pathology of subarachnoid hemorrhage likely involves major morphological changes in the microcirculation. However, previous studies primarily used fixed tissue or delayed injury models. Therefore, in the present study, we used *in vivo* imaging to observe the dynamic changes in cerebral microcirculation after subarachnoid hemorrhage. Subarachnoid hemorrhage was induced by perforation of the bifurcation of the middle cerebral and anterior cerebral arteries in male C57/BL6 mice. The diameter of pial arterioles and venules was measured by *in vivo* fluorescence microscopy at different time points within 180 minutes after subarachnoid hemorrhage. Cerebral blood flow was examined and leukocyte adhesion/albumin extravasation was determined at different time points before and after subarachnoid hemorrhage. Cerebral pial microcirculation was abnormal and cerebral blood flow was reduced after subarachnoid hemorrhage. Acute vasoconstriction occurred predominantly in the arterioles instead of the venules. A progressive increase in the number of adherent leukocytes in venules and substantial albumin extravasation were observed between 10 and 180 minutes after subarachnoid hemorrhage. These results show that major changes in microcirculation occur in the early stage of subarachnoid hemorrhage. Our findings may promote the development of novel therapeutic strategies for the early treatment of subarachnoid hemorrhage.

Key Words: *nerve regeneration; subarachnoid hemorrhage; microcirculation disturbance; leukocyte adhesion; albumin extravasation; cerebral blood flow; vasoconstriction; early brain injury; neural regeneration*

Introduction

Subarachnoid hemorrhage (SAH) accounts for 2–9% of strokes and is associated with high morbidity and mortality (Fujii et al., 2013). Delayed vasospasm that develops within 3–7 days after SAH is widely considered an important cause of poor outcome (Jia et al., 2009). Although animal studies have led to the identification of many agents that inactivate spasmogenic substances or block arterial smooth muscle contraction, no drug has been successful in improving clinical outcome after SAH (Okada and Suzuki, 2017). Moreover, clinical trials have shown that reducing delayed vasospasm does not significantly improve long-term prognosis (Sehba et al., 2011). For this reason, early brain injury within the first 72 hours after SAH has re-attracted the attention of researchers (Chen et al., 2014) and is now considered a major cause of poor prognosis (contributing to 30–70% mortality). Because key pathological events are thought to be initiated within minutes after aneurysmal SAH (Ostrowski et al.,

2006), our experiments focused on the early stage after SAH. The pathological mechanisms contributing to brain injury include acute cerebral vasoconstriction, increased intracranial pressure, microcirculatory disturbance, oxidative stress, the immune inflammatory response, and cellular apoptosis and death (Kozniewska et al., 2006; Hansen-Schwartz et al., 2007). After the rupture of an intracranial aneurysm, intracranial pressure rises rapidly, quickly hindering intracranial circulation. This event promotes hemostasis and leads to a reduction in cerebral perfusion pressure and cerebral blood flow (Kozniewska et al., 2006; Liu et al., 2017).

To date, most studies on SAH have used fixed tissue (Sehba et al., 2005, 2007) to examine acute (within 2 hours) changes in the diameter of big vessels or alterations in microcirculation (Sun et al., 2009). Only limited data are available on the microcirculatory changes after SAH *in vivo* (Friedrich et al., 2012). Therefore, in the present study, we used *in vivo* microscopy to investigate the changes in pial microcirculation up to 180 minutes after SAH. We also evaluated potential dynamic interactions between cerebral blood flow, thrombus formation, cerebral microconstriction and albumin extravasation, in an effort to provide insight into the mechanisms responsible for early brain injury after SAH.

Materials and Methods

Animals

A total of 36 specific-pathogen-free male C57/BL6 mice, weighing 22–25 g and 8 weeks of age, were purchased from the Animal Center of Peking University Health Science Center in China (certificate No. SCXK2006-0008). The animals were raised in cages under a 12/12-hour light/dark cycle and were allowed free access to food and water. Before the experiment, the mice were fasted for 12 hours. The protocols (**Figure 1B**) were approved by the Ethics Committee of Animal Experiments of Peking University Health Science Center. Mice were randomly divided into sham and SAH groups (n = 18 per group).

Induction of SAH models

The mouse model of SAH was established according to a previously published protocol (Yang et al., 2010). Briefly, the mice were anesthetized by an intraperitoneal injection of α-chloralose (40 mg/kg) and urethane (400 mg/kg) and placed on a heating pad to maintain body temperature at 37 ± 0.5°C. For mice in the SAH group (n = 18), a nylon suture (5–0) was inserted through the internal carotid artery to perforate the bifurcation of the middle and anterior cerebral arteries. Mice in the sham group (n = 18) underwent the same procedure without perforating the artery. After the surgery, mice were allowed to recover and given free access to food and water.

Measurement of cerebral blood flow

A laser Doppler perfusion imaging system (PeriScan PIM3 System; PERIMED, Stockholm, Sweden) was used to measure cerebral blood flow, as described previously (Huang et al., 2012). The skull was exposed, and a computer-controlled optical scanner-directed He/Ne laser beam was placed 18–19 cm above the exposed cerebral cortex. The beam illuminated the cortex to a depth of 0.5 mm. The images were acquired before SAH or sham surgery and at 10, 20, 30, 60, 120 and 180 minutes after SAH or sham surgery. Relative perfusion values were normalized and shown as a percentage of the levels before SAH and before sham surgery. A decrease in cerebral blood flow was considered to indicate a successful SAH procedure (Naraoka et al. 2014).

Microcirculatory monitoring

Figure 1A shows the cranial window (2 mm × 2 mm) situated 1 mm lateral to the bregma over the right anterior of the parietal cortex with the dura mater intact. NaCl (0.9%, 37°C) was gently perfused over the exposed dura mater to maintain physiological conditions. We randomly selected at least three venules (diameter: 20–100 μm) and three arterioles (diameter: 20–100 μm) for analysis. The same part of each vessel was observed before and after SAH. Each part was evaluated for 15 seconds at the different time points. Images were recorded and analyzed in a double-blind manner. The changes in microcirculation were observed for 180 minutes using a biological microscope (DM-LFS, Leica, Wetzlar, Germany) equipped with a video timer (VTG-55B, For-A, Tokyo, Japan), a color monitor (J2118A, TCL, Huizhou, China) and a DVD recorder (DVR-R25, Malata, Xiamen, China). The images were recorded by a high-speed video camera system (Fastcam-ultima APX, Photron, San Diego, CA, USA).

Measurement of albumin extravasation

We observed albumin extravasation with an upright fluorescence microscope (BX51, Olympus, Tokyo, Japan). The cerebral venules (35–45 μm in diameter) were selected for observation. Mice (n = 6) with inflammatory process or bleeding in the cranial window were excluded. The mice were injected with 50 mg/kg fluorescein isothiocyanate (FITC)-albumin (Sigma-Aldrich, St. Louis, MO, USA) intravenously through the femoral vein 10 minutes before observation. The fluorescence signal (emission wavelength of 520 nm and an excitation wavelength of 490 nm) was acquired using a super-sensitive CCD camera (USS-301, UNIQ Vision Inc, Santa Clara, CA, USA). Albumin extravasation was expressed as Ii/Iv (where Ii represents the fluorescence intensity of FITC-albumin in the perivenular interstitial area and Iv represents the fluorescence intensity of FITC-albumin in the venules) (Xu et al., 2009; Wang et al., 2012).

Measurement of adherent leukocytes

Rhodamine 6G (5 mg/kg, Sigma-Aldrich) was administrated *via* the femoral vein after craniotomy, and the venules were observed before and after surgery at the different time points (10, 20, 30, 60, 120 and 180 minutes) (n = 6). The cerebral microvenules (35–45 μm in diameter) were selected for observation. The microvessels were observed under an upright

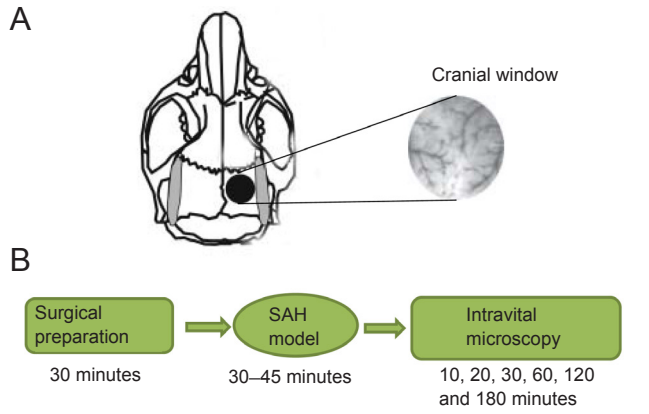

Figure 1 Diagrammatic sketch of the cranial window and experimental protocol.
(A) Diagrammatic sketch of the location of the cranial window used for intravital microscopy. (B) Experimental protocol. Mice were re-anesthetized at different time points for intravital microscopy after SAH. SAH: Subarachnoid hemorrhage.

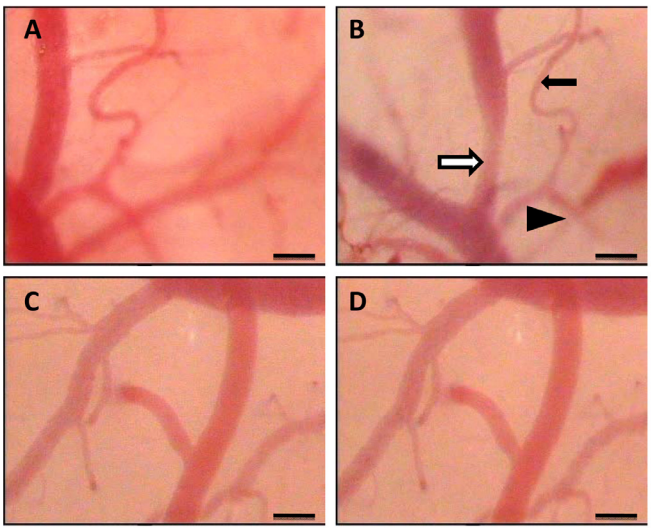

Figure 3 Microvascular constriction observed by a high-speed video camera system.
(A) Blood vessels before SAH. (B) Three hours after SAH, arteriolar constrictions varied, but were present in the main branches (white arrow), median-sized branches (black arrowhead) and small vessels (black arrow), with constrictions of 10–40%. (C, D) No microvascular constrictions were observed in the venules. (C) Venules before SAH. (D) Venules after SAH. Scale bars: 20 μm. SAH: Subarachnoid hemorrhage.

fluorescence microscope (DM-LFS, Leica) using a helium-neon laser beam for illumination after craniotomy. The adherent leukocytes were identified as those that attached to the venular walls for more than 30 seconds. The number of adherent leukocytes was scored before and 10, 20, 30, 60,120 and 180 minutes after SAH (Xu et al., 2009; Huang et al., 2012).

Statistical analysis

Data are presented as the mean ± SEM and were analyzed with SPSS software (Version22.0, IBM, Armonk, NY, USA). The Mann-Whitney *U* test was used for the analysis of differences between different time points. A value of $P < 0.05$ was considered statistically significant.

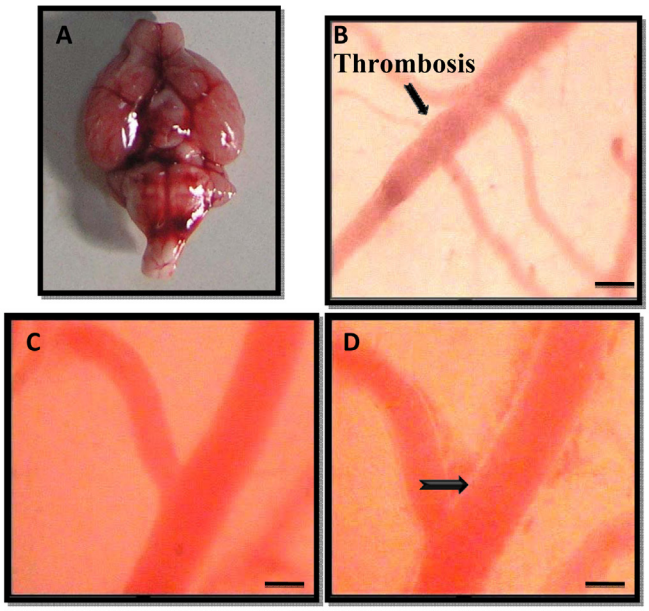

Figure 2 Blood distribution and thrombosis after SAH observed with a high-speed video camera.
(A) Three hours after SAH, a blood clot (arrows) was observed around the cisterna magna, basilar cistern and basilar artery at the base of the skull. (B) The thrombosis formed 120 minutes after SAH. The arrow points to the thrombosis after the induction of SAH. (C, D) The same blood vessel before SAH and 30 minutes after SAH. The blood accumulated around vessels after SAH viewed as a light margin ensheathing the vessels in the subarachnoid space (black arrow in D). The images were recorded by a high-speed video camera system. Scale bars: 20 μm. SAH: Subarachnoid hemorrhage.

Results

Blood distribution after SAH

Blood accumulated in the subarachnoid space 3 hours after SAH at the base of the skull (**Figure 2A**). After SAH, the formation of thrombi, as shown in **Figure 2B**, in the arterioles constricted blood flow in the microvascular system. Three hours after SAH, only a few thrombi were observable. **Figure 2C** shows blood vessel before SAH. The blood did not distribute evenly, but accumulated around vessels, observable as a light margin around the vessels in the subarachnoid space (black arrow; **Figure 2D**).

Microvascular constriction

During the 3 hours after SAH, we observed numerous constricted microvessels. All constricted vessels were arterioles, and no constriction was observed in the venules (**Figure 3**). **Figure 3A** shows the vessels before SAH and 3 hours after SAH. Arteriolar constrictions varied, but the main branches (white arrow), median-sized branches (black arrow head) and smaller vessels (black arrow) were constricted by 10–30%. This differs from the pearl string-like constrictions observed in SAH patients in another study (Uhl et al., 2003; Friedrich et al., 2012). We did not find any microvascular

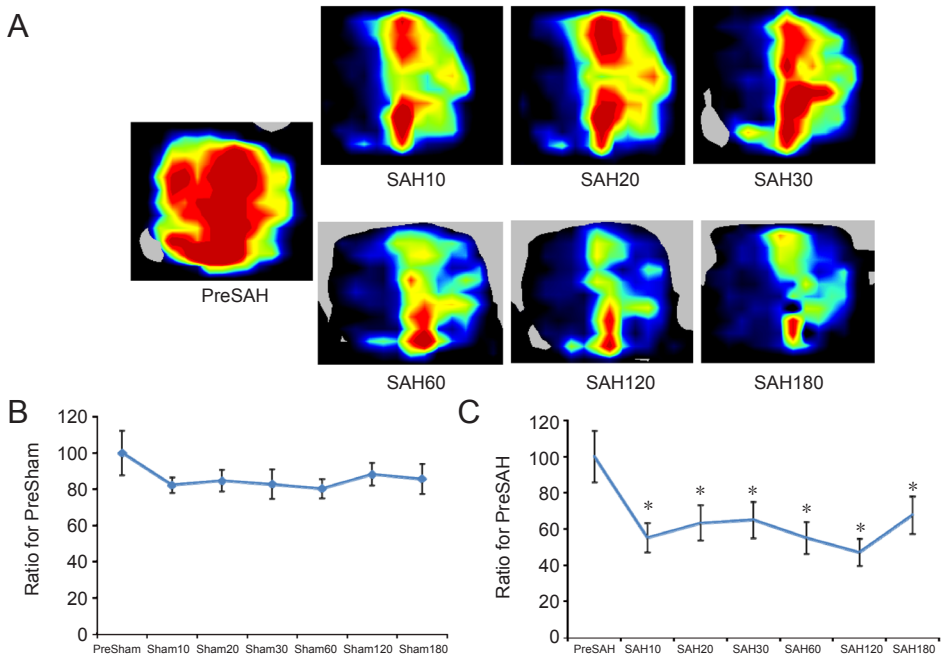

Figure 4 Cerebral blood flow (CBF) on the cortex observed through a cranial window.

(A) Representative images of cortical CBF at different time points, acquired with a laser Doppler perfusion imaging system. The different colors indicate the amount of CBF, with red to blue denoting high to low. (B) Quantitative analysis of CBF at different time points in the sham group. There was no significant difference between the time point prior to sham surgery (PreSham) and the different time points after the sham surgery. (C) Quantitative analysis of CBF at the different time points in the SAH group. After SAH, the CBF was significantly reduced at the different time points, compared with the time point prior to SAH (preSAH). Data are presented as the mean ± SEM (n = 6). $*P < 0.05$, *vs.* PreSAH. 10, 20, 30, 60, 120 and 180 indicate the minutes after sham surgery or SAH. SAH: Subarachnoid hemorrhage.

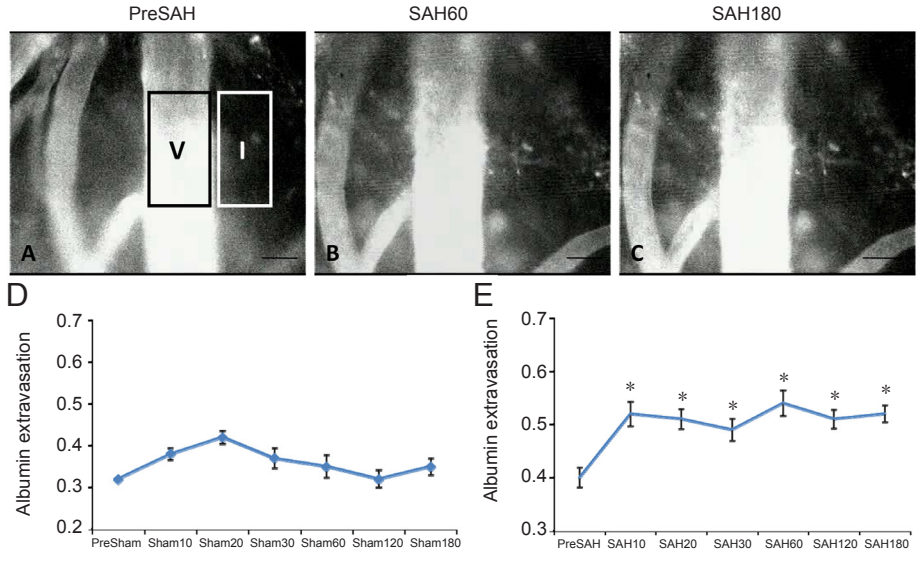

Figure 5 Albumin extravasation in the brain of mice after SAH.

(A) Representative images of the extravasation of albumin from venules before SAH (upright fluorescence microscope). Rectangle (I) indicates interstitial tissue. Image in rectangle (V) is that of a cerebral venule. (B) Albumin extravasation 60 minutes after SAH. (C) Albumin extravasation 180 minutes after SAH. Scale bars: 20 μm in A–C. (D) Statistical analysis of albumin extravasation in the sham group. There are no significant differences between the time point prior to sham surgery (PreSham) and the various time points after sham surgery. (E) Statistical analysis of albumin extravasation. Albumin extravasation was significantly increased at the different time points after SAH compared with before SAH. Albumin extravasation is presented as Ii/Iv (Ii represents the fluorescence intensity of FITC-albumin in the perivenular interstitial area and Iv represents the fluorescence intensity of FITC-albumin in the venules). Data are the mean ± SEM (n = 6). $*P < 0.05$, *vs.* preSAH. 10, 20, 30, 60, 120 and 180 indicate the minutes after sham surgery or SAH. SAH: Subarachnoid hemorrhage; FITC: fluorescein isothiocyanate.

constrictions in the venules (**Figure 3C, D**).

Cerebral blood flow changes after SAH

Using the laser Doppler perfusion imaging system, we observed cerebral blood flow changes at different time points (**Figure 4A**). The data were quantified and are shown for the SAH group in **Figure 4C**. Notably, SAH induced a severe reduction in cerebral blood flow, compared with before SAH, and this reduction was maintained for 3 hours. There were no significant changes before and after sham surgery (**Figure 4B**).

Albumin extravasation

Figure 5A–C shows the transvascular efflux of FITC-labeled albumin from the cerebral venules, and **Figure 5E** shows the quantification of these data before and after SAH at the different time points. A slight fluorescence was observed in the interstitial tissue outside the venule before SAH. Albumin extravasation increased significantly 10 minutes after SAH, and persisted at a high level until 3 hours after SAH (**Figure 5E**). There were no significant changes in albumin extravasation before and after sham surgery (**Figure 5D**).

Adherent leukocytes after SAH

Figure 6A shows leukocytes adhering to venular walls after SAH. The quantitative analysis of the number of adherent leucocytes at the different time points is shown in **Figure 6B**

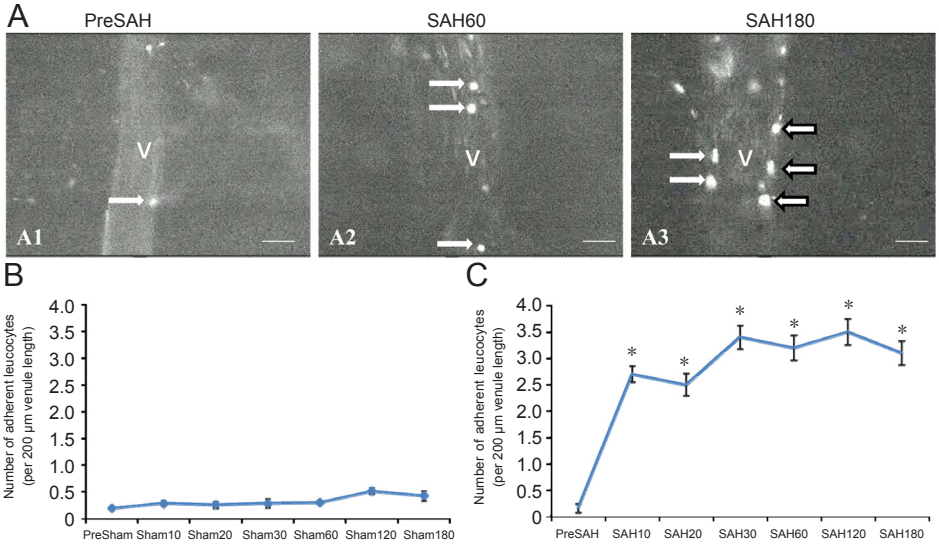

(A) Venular wall acquired at baseline (PreSAH) (A1) and 60 minutes (A2) and 180 minutes (A3) after SAH (upright fluorescence microscope). White arrows indicate the adherent leukocytes. Scale bars: 20 μm. V: Venule. (B) Statistical analysis of the number of adherent leucocytes at the different time points in the sham group. No significant changes were observed between preSham and the different time points after sham surgery. (C) Time course of the number of adherent leucocytes at the different time points. Compared with preSAH, the number of adherent leukocytes increased significantly starting 10 minutes after SAH injury. No significant changes were observed among the different time points after SAH. Data are presented as the mean ± SEM (n = 6). $*P < 0.05$, *vs.* PreSAH. PreSham: Before sham surgery; PreSAH: before SAH. 10, 20, 30, 60, 120 and 180 indicate the minutes after sham surgery or SAH. SAH: Subarachnoid hemorrhage.

Figure 6 Leukocytes adherent on the venular walls in mice after SAH.

and C. There were no significant changes between the different time points after surgery or before sham surgery (**Figure 6B**). However, the number of adherent leukocytes increased significantly starting 10 minutes after SAH compared with before SAH (**Figure 6C**). There were no significant changes in the number of adherent leukocytes between the different time points after SAH.

Discussion

In the present study, *in vivo* imaging was used to investigate changes in cerebral microcirculation after experimental SAH in mice. Cerebral pial microcirculation was evaluated for 3 hours after operation. SAH induced arteriolar constrictions, cerebral blood flow reductions, substantial albumin extravasation and an increase in adherent leukocytes in venules. These changes might contribute to early brain injury after SAH.

SAH patients might suffer cerebral ischemia after hemorrhage, although large blood vessel spasm is not detected angiographically (Uhl et al., 2003; Schubert et al., 2009). Despite scarce clinical evidence, microcirculatory changes and early perfusion disturbances have been reported in some studies (Ohkuma et al., 2000, 2001). In the present study, limited to 3 hours after acute SAH, arteriolar constriction by over 60% was observed in the main, median-sized and small branches, indicating that the constriction happens soon after ischemia (within 10 minutes). These findings are similar to those in human patients (Uhl et al., 2003; Pennings et al., 2004, 2009) and mice (Friedrich et al., 2012), although the timing of early brain injury was no less than 24 hours in humans and 3 hours in mice in those previous studies. Therefore, in the present study, we investigated changes at a very early stage, and showed that constriction of arterioles appears rapidly after SAH. In contrast to a study in rats which suggested that constriction of arterioles and venules occurs acutely after SAH (*i.e.*, 5 minutes) *in vivo* (Sun et al., 2009), we found no signs of constricted venules in our current study using mice.

The constriction of arterioles resulted in a significant reduction in cerebral blood flow shortly after SAH, indicating that the model was successfully induced. Assuming that vessels are rigid bodies, according to the Poiseuille law, tubular constriction by over 60% will lead to a reduction in the quantity of flow by 13%. Therefore, the microconstriction itself is able to cause a substantial decrease in cerebral blood flow in the early phase of SAH. Furthermore, a decrease in nitric oxide after SAH in animal models and humans has been observed (Schwartz et al., 2000; Sehba and Bederson, 2011). It strongly affects constriction at the early stage of SAH. The selective constriction of arterioles (*i.e.*, not venules) might therefore result from the larger quantity of smooth muscle cells in these vessels that can respond to the decrease in nitric oxide. It has also been claimed that cyclooxygenase-2 might be related to the pathogenesis of cerebral vasospasm through nitric oxide and ET-1 (Munakata et al., 2016). A number of different factors and mechanisms therefore appear to underlie microconstriction.

It has been reported that nitric oxide produced by endothelial nitric oxide synthase is important for vascular functions, such as the regulation of vascular tone and adhesion of leukocytes to the endothelium (Cooke and Dzau, 1997), which contribute to early brain injury (Cossu et al., 2014). During inflammation, there is an increase in the expression of adhesion molecules in the endothelium of the cerebral microvasculature, including vascular adhesion molecule-1, intercellular adhesion molecule-1, E-selectin and P-selectin (Ley, 1996), leading to leukocyte adhesion. Leukocyte adhesion in cerebral venules has also been observed previously in several models of ischemia/reperfusion (Ishikawa et al., 2004, 2009), supporting our results. In our present study, albumin extravasation and leukocyte adhesion to venular walls occurred simultaneously, suggesting that these two

processes are related. Neutrophils were observed to adhere to the cerebral venules within 10 minutes after SAH in rats (Friedrich et al., 2011). Reactive oxygen species and proteinases are released by adherent neutrophils and target the basement membrane and endothelium, resulting in albumin extravasation and increased vascular permeability (Kurose et al., 1997; Olanders et al., 2002). Furthermore, free radicals activate the nuclear transcription factor NF-κB, which increases leukocyte accumulation in vessels and up-regulates the expression of intercellular adhesion molecule-1 on endothelial cells (Olanders et al., 2002). This positive feedback might contribute to the rapid increase in vascular permeability and albumin extravasation. These inflammatory processes within the first 3 hours cause early brain injury.

Platelet-leukocyte-endothelial cell interactions have been observed in the postcapillary venules on the cerebral surface immediately after SAH (Ishikawa et al., 2009). Platelet aggregation precedes thrombosis after endothelial damage. The frequency of microconstriction is greater than that of microthrombosis. The formation of thrombi could affect microvascular flow after SAH. Therefore, thrombi appear to be formed after vasoconstriction, as supported by scanning electron microscopy (Sabri et al., 2012, 2013).

Morphologically, a light margin ensheathing vessels in the subarachnoid space was observed after SAH. The vessel wall is clearly visible, contrasting with erythrocytes and hemoglobin. It has been suggest that structural changes, including endothelial and smooth muscle intima proliferation and collagenous changes, contribute to the thickening of the vessel walls (Uhl et al., 2003). These endothelial changes might decrease the diameter of vessels (Plesnila, 2013). Pearl-string-like constrictions are observed in SAH patients (≥ 24 hours) (Uhl et al., 2003; Pennings et al., 2004, 2009) and mice (≥ 3 hours) (Friedrich et al., 2012). Changes in cerebrospinal fluid flow might also occur, but the underlying mechanisms remain unclear. In our experiment, however, only a few thrombi were observable. Nevertheless, microthrombi have previously been observed in the cerebral microcirculation, occluding the proximal part of the spasm, characteristic of SAH (Tso and Macdonald, 2013). This suggests an intimate relationship between arteriolar constriction and thrombosis.

The design of this study focused on the morphology of the microcirculation and its dynamic changes. We assessed the circulatory changes in the brain through a surgical window, which might have affected the observations, particularly as the cranial window could impact intracranial pressure and influence microcirculation. In the clinical setting, nuclear medicine, magnetic resonance imaging (MRI) and X-ray computed tomography are able to assess cerebral blood flow less invasively (Griffiths et al., 2001). Among these, MRI is widely used in animals because it provides non-invasive structural, physiological and functional imaging data of the whole brain in a longitudinal manner (Sun et al., 2016). Additionally, newer optical imaging techniques, including laser speckle contrast imaging, two-photon microscopy, optical coherence tomography and diffuse correlation spectroscopy, provide high spatial and temporal resolution, and are therefore increasingly used to investigate blood flow changes (Devor et al., 2012). Therefore, to examine the links between early brain damage and dynamic microcirculatory changes induced by SAH, future studies need to focus on the associated molecular changes, ideally using one or more of these less invasive and highly-sensitive approaches.

In conclusion, we performed an *in vivo* microscopy study on the cerebral circulation at early time points after SAH in mice (up to 3 hours). We found decreased cerebral blood flow, increased thrombus formation, adherent leukocytes and albumin extravasation at the early stage. Major dynamic changes in cerebral pial microcirculation were observed in our study. Our findings should help scholars to develop targeted neuroprotective strategies for early brain injury.

Author contributions: *XMY contributed to animal model establishment, data collection and assembly, analysis and interpretation, and drafting of the paper. XHC analyzed and interpreted the data and drafted the paper. JFL collected and assembled the data. CMZ, JYH and CHC contributed to study conception and design, technique support and drafting of the paper. All authors approved the final version of this paper.*
Conflicts of interest: *None declared.*
Financial support: *This study was supported by the National Natural Science Foundation of China, No. 81100856.*
Research ethics: *The study protocol was approved by the Ethics Committee of Peking University Health Sciences Center with the Guidelines for the Use of Animals in Neuroscience Research by the Society for Neuroscience (Beijing, China).*
Data sharing statement: *Datasets analyzed during the current study are available from the corresponding author on reasonable request.*
Plagiarism check: *Checked twice by iThenticate.*
Peer review: *Externally peer reviewed.*

References

Chen S, Feng H, Sherchan P, Klebe D, Zhao G, Sun X, Zhang J, Tang J, Zhang JH (2014) Controversies and evolving new mechanisms in subarachnoid hemorrhage. Prog Neurobiol 115:64-91.

Cooke JP, Dzau VJ (1997) Nitric oxide synthase: role in the genesis of vascular disease. Annu Rev Med 48:489-509.

Cossu G, Messerer M, Oddo M, Daniel RT (2014) To look beyond vasospasm in aneurysmal subarachnoid haemorrhage. Biomed Res Int 2014:628597.

Devor A, Sakadzic S, Srinivasan VJ, Yaseen MA, Nizar K, Saisan PA, Tian P, Dale AM, Vinogradov SA, Franceschini MA, Boas DA (2012) Frontiers in optical imaging of cerebral blood flow and metabolism. J Cereb Blood Flow Metab 32:1259-1276.

Friedrich B, Muller F, Feiler S, Scholler K, Plesnila N (2012) Experimental subarachnoid hemorrhage causes early and long-lasting microarterial constriction and microthrombosis: an in-vivo microscopy study. J Cereb Blood Flow Metab 32:447-455.

Friedrich V, Flores R, Muller A, Bi W, Peerschke EI, Sehba FA (2011) Reduction of neutrophil activity decreases early microvascular injury after subarachnoid haemorrhage. J Neuroinflammation 8:103.

Fujii M, Yan J, Rolland WB, Soejima Y, Caner B, Zhang JH (2013) Early brain injury, an evolving frontier in subarachnoid hemorrhage research. Transl Stroke Res 4:432-446.

Griffiths PD, Hoggard N, Dannels WR, Wilkinson ID (2001) In vivo measurement of cerebral blood flow: a review of methods and applications. Vasc Med 6:51-60.

Hansen-Schwartz J, Vajkoczy P, Macdonald RL, Pluta RM, Zhang JH (2007) Cerebral vasospasm: looking beyond vasoconstriction. Trends Pharmacol Sci 28:252-256.

Huang P, Zhou CM, Qin H, Liu YY, Hu BH, Chang X, Zhao XR, Xu XS, Li Q, Wei XH, Mao XW, Wang CS, Fan JY, Han JY (2012) Cerebralcare Granule(R) attenuates blood-brain barrier disruption after middle cerebral artery occlusion in rats. Exp Neurol 237:453-463.

Ishikawa M, Cooper D, Arumugam TV, Zhang JH, Nanda A, Granger DN (2004) Platelet-leukocyte-endothelial cell interactions after middle cerebral artery occlusion and reperfusion. J Cereb Blood Flow Metab 24:907-915.

Ishikawa M, Kusaka G, Yamaguchi N, Sekizuka E, Nakadate H, Minamitani H, Shinoda S, Watanabe E (2009) Platelet and leukocyte adhesion in the microvasculature at the cerebral surface immediately after subarachnoid hemorrhage. Neurosurgery 64:546-553.

Jia L, Sun BL, Zhang L (2009) Establishment of an animal model of cerebral vasospasm following subarachnoid hemorrhage. Zhongguo Zuzhi Gongcheng Yanjiu 13:8147-8150.

Kozniewska E, Michalik R, Rafalowska J, Gadamski R, Walski M, Frontczak-Baniewicz M, Piotrowski P, Czernicki Z (2006) Mechanisms of vascular dysfunction after subarachnoid hemorrhage. J Physiol Pharmacol 57 Suppl 11:145-160.

Kurose I, Argenbright LW, Wolf R, Lianxi L, Granger DN (1997) Ischemia/reperfusion-induced microvascular dysfunction: role of oxidants and lipid mediators. Am J Physiol 272:H2976-2982.

Ley K (1996) Molecular mechanisms of leukocyte recruitment in the inflammatory process. Cardiovasc Res 32:733-742.

Liu JH, Li XK, Chen ZB, Cai Q, Wang L, Ye YH, Chen QX (2017) D-dimer may predict poor outcomes in patients with aneurysmal subarachnoid hemorrhage: a retrospective study. Neural Regen Res 12:2014- 2020.

Munakata A, Naraoka M, Katagai T, Shimamura N, Ohkuma H (2016) Role of cyclooxygenase-2 in relation to nitric oxide and endothelin-1 on pathogenesis of cerebral vasospasm after subarachnoid hemorrhage in rabbit. Transl Stroke Res 7:220-227.

Naraoka M, Matsuda N, Shimamura N, Asano K, Ohkuma H (2014) The role of arterioles and the microcirculation in the development of vasospasm after aneurysmal SAH. Biomed Res Int 2014:253746.

Ohkuma H, Manabe H, Tanaka M, Suzuki S (2000) Impact of cerebral microcirculatory changes on cerebral blood flow during cerebral vasospasm after aneurysmal subarachnoid hemorrhage. Stroke 31: 1621-1627.

Ohkuma H, Ogane K, Tanaka M, Suzuki S (2001) Assessment of cerebral microcirculatory changes during cerebral vasospasm by analyzing cerebral circulation time on DSA images. Acta Neurochir Suppl 77:127-130.

Okada T, Suzuki H (2017) Toll-like receptor 4 as a possible therapeutic target for delayed brain injuries after aneurysmal subarachnoid hemorrhage. Neural Regen Res 12:193-196.

Olanders K, Sun Z, Borjesson A, Dib M, Andersson E, Lasson A, Ohlsson T, Andersson R (2002) The effect of intestinal ischemia and reperfusion injury on ICAM-1 expression, endothelial barrier function, neutrophil tissue influx, and protease inhibitor levels in rats. Shock 18:86-92.

Ostrowski RP, Colohan AR, Zhang JH (2006) Molecular mechanisms of early brain injury after subarachnoid hemorrhage. Neurol Res 28: 399-414.

Pennings FA, Albrecht KW, Muizelaar JP, Schuurman PR, Bouma GJ (2009) Abnormal responses of the human cerebral microcirculation to papaverin during aneurysm surgery. Stroke 40:317-320.

Pennings FA, Bouma GJ, Ince C (2004) Direct observation of the human cerebral microcirculation during aneurysm surgery reveals increased arteriolar contractility. Stroke 35:1284-1288.

Plesnila N (2013) Pathophysiological role of global cerebral ischemia following subarachnoid hemorrhage: the current experimental evidence. Stroke Res Treat 2013:651958.

Sabri M, Ai J, Lakovic K, D'Abbondanza J, Ilodigwe D, Macdonald RL (2012) Mechanisms of microthrombi formation after experimental subarachnoid hemorrhage. Neuroscience 224:26-37.

Sabri M, Ai J, Lakovic K, Macdonald RL (2013) Mechanisms of microthrombosis and microcirculatory constriction after experimental subarachnoid hemorrhage. Acta Neurochir Suppl 115:185-192.

Schubert GA, Seiz M, Hegewald AA, Manville J, Thome C (2009) Acute hypoperfusion immediately after subarachnoid hemorrhage: a xenon contrast-enhanced CT study. J Neurotrauma 26:2225-2231.

Schwartz AY, Sehba FA, Bederson JB (2000) Decreased nitric oxide availability contributes to acute cerebral ischemia after subarachnoid hemorrhage. Neurosurgery 47:208-214.

Sehba FA, Bederson JB (2011) Nitric oxide in early brain injury after subarachnoid hemorrhage. Acta Neurochir Suppl 110:99-103.

Sehba FA, Friedrich V Jr, Makonnen G, Bederson JB (2007) Acute cerebral vascular injury after subarachnoid hemorrhage and its prevention by administration of a nitric oxide donor. J Neurosurg 106: 321-329.

Sehba FA, Mostafa G, Friedrich V Jr, Bederson JB (2005) Acute microvascular platelet aggregation after subarachnoid hemorrhage. J Neurosurg 102:1094-1100.

Sehba FA, Pluta RM, Zhang JH (2011) Metamorphosis of subarachnoid hemorrhage research: from delayed vasospasm to early brain injury. Molecular Neurobiology 43:27.

Sun BL, Zheng CB, Yang MF, Yuan H, Zhang SM, Wang LX (2009) Dynamic alterations of cerebral pial microcirculation during experimental subarachnoid hemorrhage. Cell Mol Neurobiol 29:235-241.

Sun Y, Shen Q, Watts LT, Muir ER, Huang S, Yang GY, Suarez JI, Duong TQ (2016) Multimodal MRI characterization of experimental subarachnoid hemorrhage. Neuroscience 316:53-62.

Tso MK, Macdonald RL (2013) Acute microvascular changes after subarachnoid hemorrhage and transient global cerebral ischemia. Stroke Res Treat 2013:425281.

Uhl E, Lehmberg J, Steiger HJ, Messmer K (2003) Intraoperative detection of early microvasospasm in patients with subarachnoid hemorrhage by using orthogonal polarization spectral imaging. Neurosurgery 52:1307-1315.

Wang F, Hu Q, Chen CH, Xu XS, Zhou CM, Zhao YF, Hu BH, Chang X, Huang P, Yang L, Liu YY, Wang CS, Fan JY, Zhang K, Li GY, Wang JH, Han JY (2012) The protective effect of Cerebralcare Granule(R) on brain edema, cerebral microcirculatory disturbance, and neuron injury in a focal cerebral ischemia rat model. Microcirculation 19: 260-272.

Xu XS, Ma ZZ, Wang F, Hu BH, Wang CS, Liu YY, Zhao XR, An LH, Chang X, Liao FL, Fan JY, Niimi H, Han JY (2009) The antioxidant Cerebralcare Granule attenuates cerebral microcirculatory disturbance during ischemia-reperfusion injury. Shock 32:201-209.

Yang X, Chen C, Hu Q, Yan J, Zhou C (2010) Gamma-secretase inhibitor (GSI1) attenuates morphological cerebral vasospasm in 24h after experimental subarachnoid hemorrhage in rats. Neurosci Lett 469: 385-390.

(*Copyedited by Patel B, Wysong S, Yu J, Li CH, Qiu Y, Song LP, Zhao M*)